Physical Layer Impairments in Cascaded Multi-Degree CDC ROADMs with NRZ and Nyquist Pulse Shaped Signals

Diogo G. Sequeira[1], Luís G. Cancela[1,2] and João L. Rebola[1,2]
[1]*Optical Communications and Photonics Group, Instituto de Telecomunicações, Lisbon, Portugal*
[2]*Department of Information Science and Technology, Instituto Universitário de Lisboa (ISCTE-IUL), Lisbon, Portugal*
{dgsao, luis.cancela, joao.rebola}@iscte-iul.pt

Keywords: ASE noise, broadcast and select, in-band crosstalk, Nyquist pulse, optical filtering, ROADMs, route and select.

Abstract: Nowadays, reconfigurable optical add/drop multiplexers (ROADMs) are mainly based on broadcast and select (B&S) and route and select (R&S) architectures. Moreover, the most used components to implement the colorless, directionless and contentionless (CDC) ROADM add/drop structures are the multicast switches (MCSs) and the wavelength selective switches (WSSs). In-band crosstalk, amplified spontaneous emission (ASE) noise accumulation and optical filtering are physical layer impairments (PLIs) that become more enhanced in a CDC ROADM cascade. In this work, we investigate the impact of these PLIs in a cascade of CDC ROADMs based on both B&S and R&S architectures, with MCSs and WSSs-based add/drop structures and for nonreturn-to-zero (NRZ) and Nyquist pulse shaped signals. We show that the optical filtering impairment is more limiting for a R&S architecture. We also show that the ASE noise accumulation after 32 cascaded ROADMs leads to a 10 dB optical signal-to-noise ratio (OSNR) penalty. Finally, we conclude that the in-band crosstalk introduced in CDC ROADMs based on B&S is more harmful than with a R&S architecture. An OSNR penalty of 1 dB due to in-band crosstalk, is reached after 13 and 24 cascaded 16-degree CDC ROADMs for, respectively, NRZ and Nyquist pulse shaped signals.

1 INTRODUCTION

The continuous and exponential increase of data traffic in recent years has been putting the optical network infrastructures in a constant pursuit of new technologies that can transport huge amounts of bits in a more cost effective and efficient way. Technologies, such as coherent detection, advanced digital signal processing, polarization division multiplexing (PDM) and wavelength division multiplexing (WDM) are now fundamental to achieve these goals (Roberts et al., 2017).

Moreover, as the data traffic becomes more heterogeneous in terms of bit rate and modulation format, and the connections duration decreases, a more dynamic, flexible and reconfigurable optical transport network is required (Jinno, 2017). These requirements can be provided by the optical network nodes, currently known as reconfigurable optical add/drop multiplexers (ROADMs) with colorless, directionless and contentionless (CDC) add/drop structures (Gringeri et al., 2010). The CDC ROADM nodes can express, add and drop any WDM signal without restrictions and contention of wavelengths (Feuer. et al., 2011).

The most used architectures to implement the ROADM nodes are the broadcast and select (B&S) and route and select (R&S) architectures (Simmons, 2014). The B&S is the cheapest implementation, but has higher insertion losses and poor isolation than the R&S architecture. On the other hand, the R&S architecture is the best choice in terms of isolation of adjacent channels and has low insertion losses, but since it is based on wavelength selective switches (WSSs), the filtering effects are more relevant and the cost is higher than the B&S architecture.

In a multi-degree CDC ROADM-based optical network, the physical layer impairments (PLIs), such as optical filtering, amplified spontaneous emission (ASE) noise accumulation and in-band crosstalk, limit the number of ROADM nodes that an optical signal can pass along the network (Tibuleac and Filer, 2010). These PLIs are cumulative along the network and depend not only on the ROADM architecture, e.g. B&S or R&S, but also on the ROADM add/drop structures.

In the literature, some studies were performed to address the impact of these PLIs on the network performance. In (Filer and Tibuleac, 2012), the optical filtering and in-band crosstalk impairments due to a cascade of WSSs, have been considered, but any ROADM architectures type was considered. In (Filer and Tibuleac, 2014), the impact of the B&S and R&S architectures are considered, but the influence of the ROADM add/drop structures has been neglected. In (Pan and Tibuleac, 2016), the filtering and in-band crosstalk impact were evaluated considering the 37.5 GHz flexible grid. In this study, the authors considered a colorless add/drop structure. In (Morea et al., 2015), the impact of filtering for both the 50 GHz fixed grid and 37.5 GHz flexible grid is evaluated. In this study, the crosstalk impact is not considered, as well as the contentionless ROADM feature. In all these previous studies, the ASE noise accumulation is not considered. Instead, the authors considered that the ASE noise is totally loaded at the system input (Pan and Tibuleac, 2016) or at the system output (Morea et al., 2015).

In this work, we investigate the impact of the optical filtering, ASE noise accumulation and in-band crosstalk generated inside CDC ROADMs on the network performance, through Monte-Carlo simulation. PDM-quadrature phase-shift keying (PDM-QPSK) signals at 100-Gb/s, with 25 Gbaud symbol rate, for the 50 GHz fixed grid are considered, with both nonreturn-to-zero (NRZ) and Nyquist pulse shapes with a roll-off factor (β) equal to 0.1, which is a typical value (Morea et al., 2015). This study is performed by properly modelling the ROADM nodes, considering both B&S and R&S architectures and different add/drop structures, based on multicast switches (MCSs) (Way, 2012) and WSSs (Yang et al., 2017).

This work is organized as follows. Section 2 describes the simulation model of the multi-degree CDC ROADM-based optical network. Details on the ROADM add/drop structures are provided in Subsection 2.1. In Subsection 2.2, the optical filters used to model the ROADM components are presented and characterized. The optical filtering impact is studied in Section 3, for both ROADM architectures, add/drop structures and pulse shapes signals. Section 4 investigates the in-band crosstalk level evolution in a CDC ROADM cascade also for both ROADM architectures, add/drop structures and signal shapes. In Section 5, the impact of in-band crosstalk on the network performance is evaluated. Finally, in Section 6, the conclusions of this work are provided.

2 CDC ROADM-BASED OPTICAL NETWORK MODEL

In this section, we present the simulation model of an optical network based on multi-degree CDC ROADMs, as well as, the in-band crosstalk terms generated inside these ROADMs and the ASE noise added to the primary signal along the network. Subsection 2.1 describes the ROADM add/drop structures modeling. Subsection 2.2 presents the optical filters used to model the ROADM components.

Figure 1 depicts the simulation model of an optical network based on multi-degree CDC ROADMs. The red line in this figure represents the light-path of the primary signal (i.e., the signal that is taken as a reference to study the impact of the PLIs), S_{in}, since it is added to the network, in the first ROADM node, until it is dropped, in the M^{th} ROADM, $S_{o,M}$. Throughout this work, we consider a 100-Gb/s NRZ or Nyquist pulse shaped signal and QPSK modulation for the primary signal.

Regarding the in-band crosstalk signals originated along the ROADM-based optical network, we consider that all interfering signals have the same modulation format and bit rate as the primary signal, but with different arbitrary transmitted symbols, characterized by a phase difference and a time misalignment between the primary signal and in-band interferers (Cancela et al., 2016). These interfering signals arise from the ROADM inputs and from the ROADM add structures, denominated, respectively, $X_{M,inR}$ and $X_{M,addR}$, with M indicating the ROADM node and R the ROADM degree in which they are originated. In the ROADM inputs and ROADM add structures, the interfering signals pass through the respective components (e.g. WSS) and then are added to the primary signal.

Concerning the ASE noise addition, our simulation model considers that the ASE noise is added both at the ROADM inputs and outputs. The optical amplifier (OA) at the ROADM inputs is used to compensate the optical path losses, whereas the OA at the ROADM outputs is used to compensate the losses inside the ROADM node (Zami, 2013). In the simulator, we consider that all OAs impose the same optical signal-to-noise ratio (OSNR). The OSNR presented in the figures throughout this work corresponds to the OSNR imposed at the output of each OA. The ASE noise is considered as an additive white Gaussian noise.

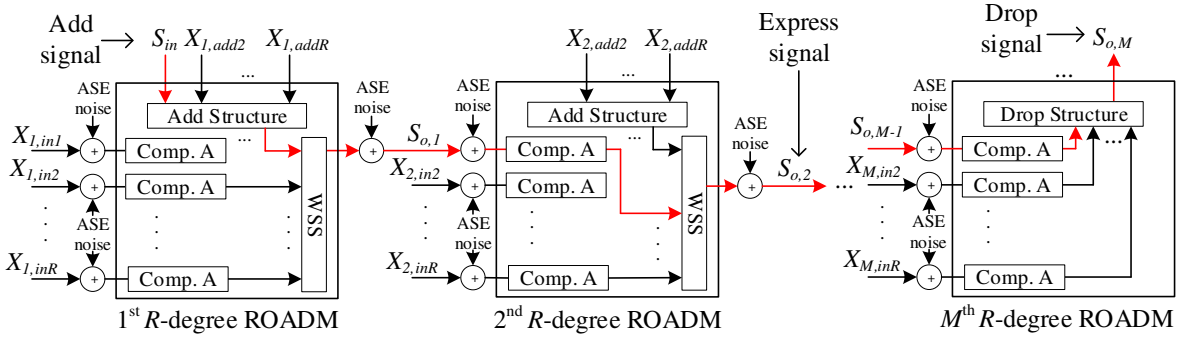

Figure 1: Simulation model of an optical network based on M cascaded R-degree CDC ROADMs.

To drop the primary signal, in the last ROADM, we use an ideal coherent detection receiver model (Essiambre et al., 2010). Consequently, our studies are done only for a single polarization, a 50-Gb/s QPSK signal, which corresponds to a 25 Gbaud symbol rate. Note that, the results for both polarizations, resulting in a 100-Gb/s QPSK signal, would be the same, since we are assuming an ideal optical receiver (Seimetz and Weinert, 2006).

As can be observed in Figure 1, at the ROADM inputs, the signals pass through Component A, which depends on the architecture used. In ROADM nodes based on a B&S architecture, Component A is an optical splitter, while with a R&S architecture, this optical splitter is replaced by a WSS. In both architectures, at the ROADM outputs, the signals go through to a WSS (Simmons, 2014). In Figure 1, to simplify, we only show the output of one direction of the ROADMs, to where the primary signal is sent.

2.1 ROADM Add/Drop Structures

In our ROADM model, we consider both MCSs and WSSs-based add/drop structures. Figure 2 depicts the model used to implement the drop structure (Colbourne and Collings, 2011). Figure 2 (a) considers a $N\times M$ MCS-based drop structure and Figure 2 (b) considers a $N\times M$ WSS-based drop structures. The corresponding model for the add structures is obtained in a similar way, by just having in mind the direction of the data flow. As can be observed from Figure 2, the MCSs are based on $1\times M$ splitters and $N\times 1$ optical switches. As such, they are not wavelength selective as the WSS structures. In terms of in-band crosstalk generation, since inside a $N\times M$ WSS, the interfering signals pass through the isolation of two WSSs, the interferers are of second order, instead of the first order interferers that appear on the $N\times M$ MCSs. On the other hand, the WSS structures have higher costs and are more filtering selective than the MCSs. In terms of modelling these add/drop structures, the MCSs are modelled by one filtering stage, while the WSSs are modelled by two filtering stages.

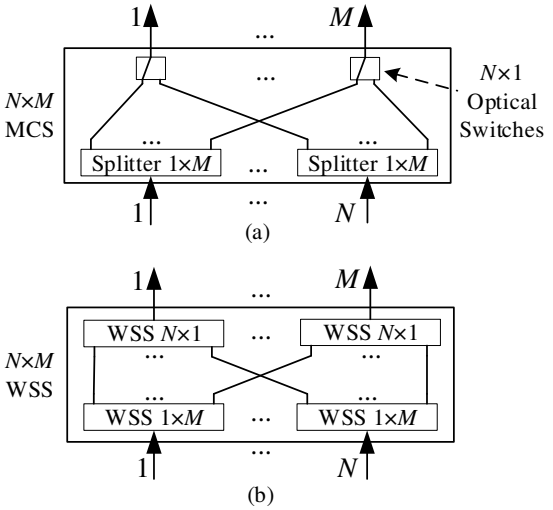

Figure 2: CDC ROADM $N\times M$ drop structures based on (a) MCSs and (b) WSSs.

2.2 Optical Filters

We consider two types of optical filters to model the ROADM components, the passband filter, $H_p(f)$, and the stopband filter, $H_b(f)$. The signals that pass through the ROADM components are filtered by the passband filter, while the interfering signals that the ROADM blocks are filtered by the stopband filter. All optical passband filters are modelled by a 4th order Super-Gaussian optical filter (Pulikkaseril, 2011) given by

$$H_p(f) = e^{-\left[\left(\frac{f}{B_0/2}\right)^{2n}\cdot\frac{\ln 2}{2}\right]} \quad (1)$$

where n is the Super-Gaussian order, B_0 is the −3 dB bandwidth, which is set to 41 GHz, usually used for the 50 GHz fixed grid (Filer and Tibuleac, 2012).

The optical stopband filters are modelled by the inversion of the optical passband filter,

$$H_b(f) = 1 - (1 - a).e^{-\left[\left(\frac{f}{B/2}\right)^{2n}.\frac{\ln 2}{2}\right]} \qquad (2)$$

where a is the blocking amplitude in linear units, $a = 10^{\frac{A\,[dB]}{20}}$. The −3 dB bandwidth of this filter, when setting B to 41 GHz, is equal to, approximately, 48 GHz. Figure 3 shows the transfer functions of these filters. Figure 3 (a) for the passband filter, $H_p(f)$, and Figure 3 (b) for the stopband filter, $H_b(f)$, with A = −40 dB.

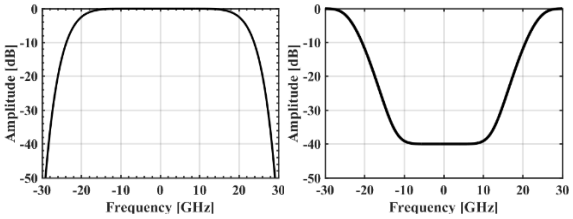

(a) (b)

Figure 3: Transfer function of the (a) 4th order Super--Gaussian optical passband filter, $H_p(f)$, and (b) optical stopband filter, $H_b(f)$, with A = −40 dB.

3 OPTICAL FILTERING IMPACT

The impact of the optical filtering in the ROADM cascade represented in Figure 1 is assessed in this section. The primary signal passes through several optical filters inside the ROADMs, before reaching its destination. These cascaded filters lead to the narrowing of the available optical bandwidth, and, consequently, to an optical OSNR penalty due to the optical filtering (Hsueh, 2012). To evaluate the OSNR penalty only due to optical filtering, i.e., the difference between the required OSNR with and without filtering impairment, we only add ASE noise at the end of the ROADM cascade, to the drop signal $S_{o,M}$ represented in Figure 1 and neglect the in-band crosstalk interferers. The bit error rate (BER) is obtained by direct-error counting, for a target value of 10^{-3}.

Figure 4 depicts the OSNR penalty due to optical filtering as a function of the number of ROADMs based on a B&S (dashed lines) and a R&S (solid lines) architectures, for both add/drop structures: WSSs (blue lines) and MCSs (red lines) and considering NRZ signals. We can conclude from this figure that the add/drop structures do not have a significant impact in terms of optical filtering. The difference between the OSNR penalty obtained with MCSs and WSSs-based add/drop structures is less than 0.15 dB. This difference corresponds to the additional filtering when the signal is added/dropped with WSSs-based add/drop structures.

Regarding the difference observed, in Figure 4, between the curves for B&S and R&S architectures, the OSNR penalty, as expected, is lower for a B&S architecture (Filer and Tibuleac, 2014), since with this architecture, the signal is not filtered at the ROADM inputs. For this architecture, an OSNR penalty of 1 dB is not reached after 32 cascaded ROADMs. For ROADMs based on a R&S architecture, penalties of ~1.5 dB are observed for 32 cascaded ROADMs. Considering a 1 dB OSNR penalty as the limit for this penalty, the signal can cross 20 and 22 ROADM nodes, respectively, with WSSs and MCSs-based add/drop structures.

The same studies have been done for Nyquist pulse shaped signals with β = 0.1. In this scenario, the optical filtering impact is very low, causing OSNR penalties lower than 0.1 dB for 32 cascaded ROADMs. This is explained by noting that the bandwidth of the Nyquist signals is, approximately, equal to symbol rate, 25 GHz, and the −3 dB bandwidth of the optical filters for the 50 GHz fixed grid is much larger than the symbol rate, 41 GHz, originating a negligible optical filtering impact, as it was also reported in (Morea et al., 2015).

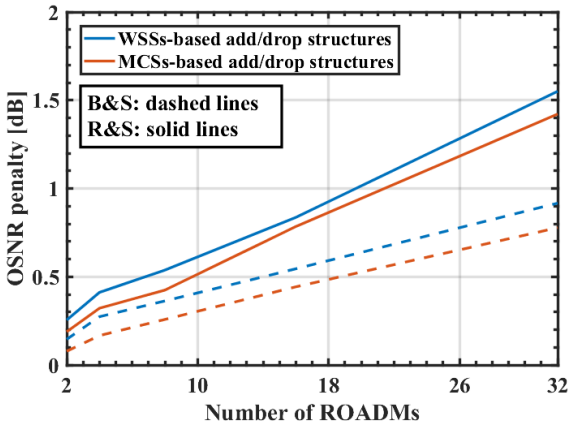

Figure 4: OSNR penalty due to optical filtering as a function of the number of ROADMs, for a BER of 10^{-3}, B&S (dashed lines) and R&S (solid lines) architectures, WSSs (blue lines) and MCSs (red lines) add/drop structures and NRZ pulse shaped signals.

4 IN-BAND CROSSTALK LEVEL IN A CDC ROADM CASCADE

In this section, the evolution of the in-band crosstalk level along a cascade of 32 CDC ROADMs is evaluated for A = −40 dB, several ROADM degrees, considering both ROADM architectures, different add/drop structures and NRZ and Nyquist pulse shaped signals. The crosstalk level, at each ROADM

output, is defined by $X_{C,M} = P_{x,M}/P_{o,M}$, where $P_{x,M}$ is the average power of all interfering signals and $P_{o,M}$ is the primary filtered signal average power, at the output of the M^{th} ROADM (Cancela et al., 2016).

Figure 5 depicts the evolution of the crosstalk level, in a cascade of 32 CDC ROADMs, as a function of the number of ROADMs based on a B&S (solid lines) and a R&S (dashed lines) architecture, considering NRZ signals. Figure 5 (a) considers MCSs and Figure 5 (b) for WSSs-based add/drop structures. Several observations can be made from this figure.

First, as expected, the crosstalk level increases with the increase of the ROADM degree.

Second, for a R&S architecture, the crosstalk level along the ROADM cascade is lower than for a B&S architecture, since, the interfering signals experience more blocking filtering stages in a R&S than in a B&S architecture.

Third observation: we can see in Figure 5 (a), with MCSs-based add/drop structures, a decrease of the crosstalk level along the network for the R&S architecture (dashed lines). This can be explained by noting that the interfering signals that came from the first ROADM add structure are considered first order crosstalk terms (i.e. they pass through one stopband filter), whereas all the other interfering terms that appear along the light-path are second order (i.e. they pass through two stopband filters). In this way, the crosstalk level of the first order terms will define the total crosstalk level behaviour, which has a decrease along the ROADM cascade because of the filtering performed by the WSSs.

On the other hand, for a B&S architecture (solid lines), the interfering terms are all first order, so the total crosstalk level increases along the ROADM cascade, except for 2-degree ROADMs. At the end of the cascade, an increase of 4 dB in the crosstalk level is observed for 16-degree ROADMs with MCSs-based add/drop structures. For 2-degree ROADMs, the crosstalk level decreases along the cascade, until the last ROADM where the crosstalk level increases. This behaviour can be explained, because there is a first order interfering term originated in the add section of the first ROADM and another originated in the ROADM input of the last ROADM. All the other ROADMs in the cascade, where the signal is expressed, do not contribute with first order interfering signals. Consequently, the ROADM filtering decreases the crosstalk level until the last ROADM, where the crosstalk level increases due to the interfering signal from the other input of the last ROADM.

Figure 5 (b) depicts the crosstalk level evolution but with WSSs-based add/drop structures. Here, we can observe a crosstalk level decreases in the last ROADM. This decrease is more abrupt for the R&S architecture, because the interfering signals pass through three stopband filters in the last ROADM node (one in the "route" WSS and two in the "drop" WSS). This crosstalk level decrease is not observed for 2-degree ROADMs based on a B&S architecture (blue solid line), for the same reason mentioned in the previous paragraph. For the R&S architecture, with WSS-based add/drop structures, the crosstalk level is practically constant along the ROADM cascade, since all interfering terms generated are second order. Consequently, the crosstalk level is, mostly, defined in the first ROADM node.

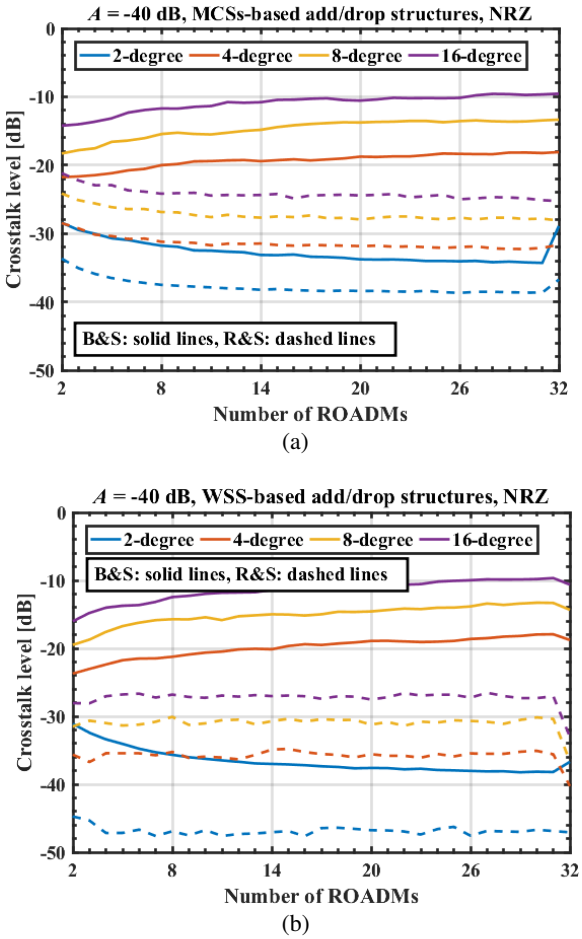

Figure 5: Crosstalk level as a function of the number of ROADMs, A = –40 dB, for both architectures, B&S (solid lines) and R&S (dashed lines), NRZ signals, several ROADM degrees and (a) MCSs and (b) WSSs-based add/drop structures.

Figure 6 shows the crosstalk level evolution along the ROADM cascade, but considering Nyquist pulse shaped signals. Figure 6 (a) refers to MCSs and Figure 6 (b) to WSS-based add/drop structures.

In Figure 6 (a), for a R&S architecture (dashed lines), a constant crosstalk level along the ROADM cascade can be observed. This behaviour is justified by the fact that the interfering terms from the first

ROADM add structure are first order terms, while the other interfering terms coming from the other ROADMs in the cascade, either from the ROADM inputs or from ROADM add structure, are all second order terms. Besides that, since the optical stopband filter in the first ROADM is more effective with Nyquist signals than with NRZ signals, the crosstalk level remains constant along the ROADM cascade.

For a B&S architecture (solid lines), the behavior of the crosstalk level evolution along the optical network is similar with the previously obtained for NRZ pulse shaped signals. Nevertheless, the crosstalk level variation between the first and the last ROADM of the cascade, in this case, is higher than with NRZ signals. For example, for 16-degree ROADM based on a B&S architecture with MCSs-based add/drop structures, we have a variation of ~11 dB and ~4 dB, respectively, for Nyquist and NRZ pulse shaped signals. The main reason is because the stopband filters used in this work, for the 50 GHz fixed grid, provide a better blocking of in-band crosstalk interfering signals for the Nyquist pulse shaped signals, since the Nyquist signals bandwidth with β = 0.1 is, approximately, one half in comparison with the NRZ signals bandwidth. For the same reason, for Nyquist pulse shaped signals, we can observe that after two cascaded ROADMs based on a B&S architecture and with MCSs-based add/drop structures, Figure 6 (a), the crosstalk level is lower ~10 dB than for NRZ pulse shaped signals, Figure 5 (a).

From Figure 6 (b), we can conclude that, with WSSs-based add/drop structures, a R&S architecture (dashed lines) and Nyquist pulse shaped signals, the crosstalk levels originated are very low, below −50 dB. For a B&S architecture (solid lines), the crosstalk levels obtained are very similar with those obtained with MCSs-based add/drop structures in Figure 5 (a).

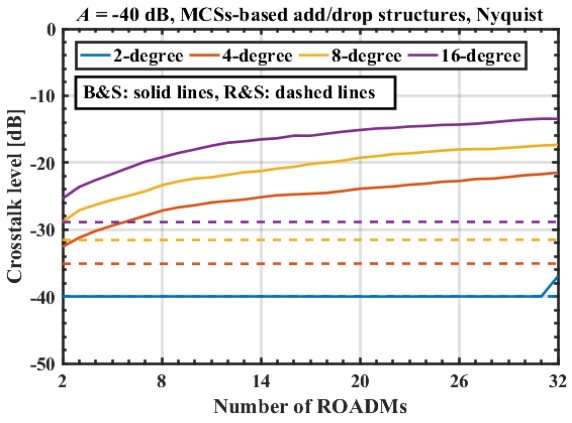

(a)

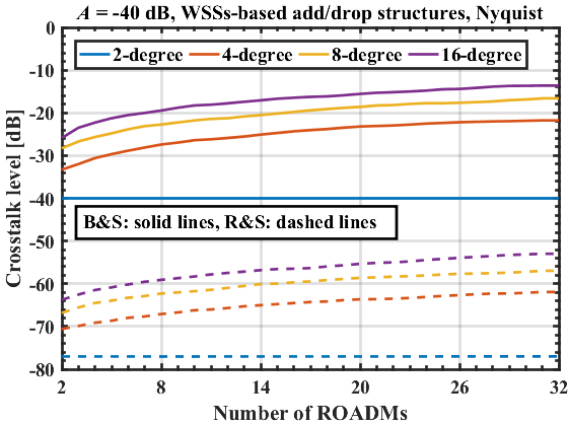

(b)

Figure 6: Crosstalk level as a function of the number of ROADMs, A = −40 dB, for both architectures, B&S (solid lines) and R&S (dashed lines), Nyquist pulse shaped signals, several ROADM degrees and (a) MCSs and (b) WSSs-based add/drop structures.

5 IN-BAND CROSSTALK IMPACT

After having studied the crosstalk level generated in a CDC ROADM cascade, for both B&S and R&S architectures, MCSs and WSSs-based add/drop structures, NRZ and Nyquist pulse shaped signals and several ROADM degrees, the OSNR penalty due to in-band crosstalk considering the model represented in Figure 1 is evaluated in this section.

In the previous section, we have concluded that with a R&S architecture, the crosstalk levels generated along the ROADM cascade are below −20 dB, and consequently, do not lead to a significant network degradation. Thus, in this section, we only study the OSNR penalty due to the in-band crosstalk for the B&S architecture.

Figure 7 shows the required OSNR, at the output of each OA, for a target BER of 10^{-3}, as a function of the number of ROADMs for NRZ (solid lines) and Nyquist (dashed lines) pulse shaped signals and a B&S architecture. The same studies have been done for the R&S architecture and the required OSNRs obtained are very similar, with differences below 0.5 dB. Note that, in this work, we consider that the required OSNR is the OSNR imposed in each OA to reach a target BER of 10^{-3}. This required OSNR is measured without the in-band crosstalk impairment, but including the impact of the optical filtering and ASE noise addition in all ROADM inputs and outputs, as shown in Figure 1.

From Figure 7, we can conclude that, the required OSNR variation with the number of ROADMs and the ROADMs degree is very similar

for both signal pulse shapes. For Nyquist pulse shaped signals, there is an improvement of the required OSNR that reaches 1 dB for 16-degree ROADMs. For all ROADM degrees considered, there is a degradation of about 10 dB of the required OSNR from a cascade of 2 nodes to a cascade of 32 ROADMs nodes. For example, for 2-degree ROADMs, the required OSNR after 2 nodes is 19 dB and after 32 nodes, it is approximately 29 dB, for NRZ pulse shaped signals.

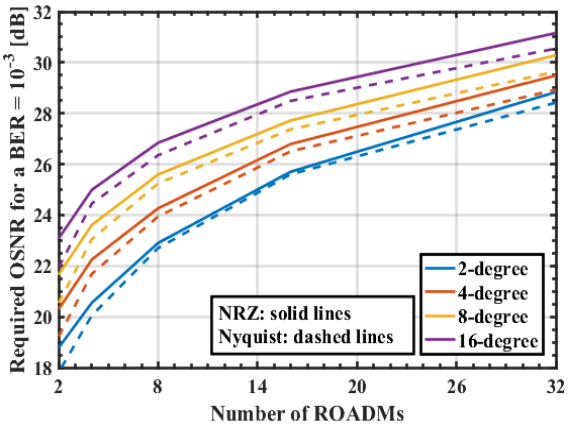

Figure 7: Required OSNR for a BER equal to 10^{-3} as a function of the number of ROADMs, for the NRZ (solid lines) and Nyquist (solid lines) pulse shaped signals, several ROADM degrees and a B&S architecture.

Figure 8 shows the OSNR penalty due to in-band crosstalk as a function of the number of ROADMs, for a target BER of 10^{-3}, $A = -40$ dB, considering both add/drop structures, MCSs (dashed lines) and WSSs (solid lines), for several ROADM degrees and NRZ pulse shaped signals. From this figure, we can conclude that, for an OSNR penalty of 1 dB, the number of cascaded ROADMs decreases with the ROADM degree increase. For example, for 8-degree ROADMs the optical signal can pass through 20 and 28 nodes, respectively, with MCSs and WSSs-based add/drop structures, while for 16-degree ROADMs, where more interfering signals arise in each node, the signal can pass through 8 and 13 ROADMs, respectively, with MCSs and WSSs-based add/drop structures. So, with the use of WSSs-based add/drop structures instead of MCSs, an improvement of 8 and 5 ROADMs has been obtained, respectively, for 8 and 16-degree ROADM degree.

Figure 9 shows the OSNR penalty due to in-band crosstalk as a function of the number of 16-degree ROADMs, for NRZ (red lines) and Nyquist (blue lines) pulse shaped signals. From this figure, we can observe a significant improvement on the ROADMs number that an optical signal can pass with the Nyquist pulse shape. An OSNR penalty of 1 dB is reached after 13 and 24 cascaded 16-degree ROADMs, for, respectively, NRZ and Nyquist pulse shaped signals with WSSs-based add/drop structures. It means an improvement of 11 ROADMs. For MCSs-based add/drop structures, the improvement is about 18 ROADMs. This improvement is related with the crosstalk level at the end of the ROADM cascade, which is higher for NRZ signals than for Nyquist pulse shaped signals, as shown in Figures 5 and 6.

Comparing the impact of the ASE noise accumulation with the in-band crosstalk impact in a CDC ROADM cascade, we can conclude that, the ASE noise accumulation has a greater impact than the in-band crosstalk in terms of OSNR penalty. As referred, at the end of a cascade with 32 ROADMs, the ASE noise accumulation leads to a OSNR penalty of, approximately, 10 dB. The in-band crosstalk, in the worst case, with NRZ pulse shaped signals, MCSs-based add/drop structures, a B&S architecture and 16-degree ROADMs, leads to a OSNR penalty slightly higher than 5 dB.

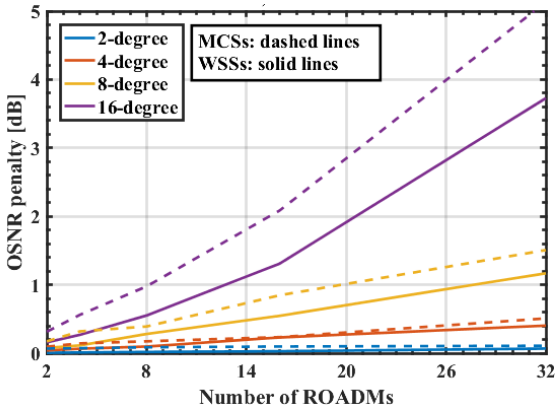

Figure 8: OSNR penalty due to the in-band crosstalk as a function of the number of ROADMs, for a BER of 10^{-3}, $A = -40$ dB, add/drop structures based on MCSs (dashed lines) and on WSSs (solid lines) and NRZ signals.

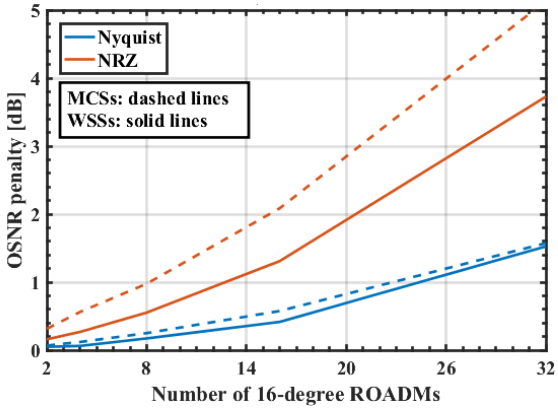

Figure 9: OSNR penalty due to in-band crosstalk as a function of the number of 16-degree ROADMs, for a BER of 10^{-3}, $A = -40$ dB, add/drop structures based on MCSs (dashed lines) and on WSSs (solid lines) and for NRZ (red lines) and Nyquist (blue lines) pulse shaped signals.

6 CONCLUSIONS

In this work, we have investigated the impact of PLIs, namely, optical filtering, in-band crosstalk and ASE noise accumulation in a CDC ROADM cascade for both B&S and R&S architectures with MCSs and WSSs-based add/drop structures. Our studies have been performed considering 100-Gb/s NRZ and Nyquist QPSK signals for the 50 GHz fixed grid.

Our results showed that the impact of the optical filtering with NRZ signals and a R&S architecture is more significant than with a B&S architecture. For CDC ROADMs based on a R&S architecture, the optical signal can pass through 20 and 22 ROADM nodes, respectively, with WSSs and MCSs-based add/drop structures, until a OSNR penalty of 1 dB is reached. The B&S architecture does not lead to a OSNR penalty of 1 dB at the end of 32 cascaded ROADMs. For Nyquist shaped signals, we have observed that the impact of optical filtering is negligible, for both ROADM architectures.

In terms of the in-band crosstalk level generated in a ROADM cascade, we have concluded that, for a R&S architecture, the crosstalk level is below –20 dB due to the enhanced signal blocking imposed by the higher number of WSSs in the light-path. In ROADMs based on a B&S architecture, the OSNR penalty due to the in-band crosstalk is higher with MCSs-based add/drop structures. An OSNR penalty of 1 dB is reached after a NRZ QPSK signal passes through 20 and 8 CDC ROADM nodes, respectively, with 8 and 16-degree. An improvement is reached using WSSs-based add/drop structures. The OSNR penalty of 1 dB due to the in-band crosstalk is reached at the end of 28 and 13 cascaded ROADMs with, respectively, 8 and 16-degree. For Nyquist pulse shaped signals, the OSNR penalty is lower than for NRZ signals, for both add/drop structures. Our results showed an improvement of 18 and 11 ROADMs with Nyquist pulse shapes for 16-degree ROADMs, and, respectively, MCS and WSSs-based add/drop structures.

We, also, have seen that, the ASE noise accumulation along the ROADM cascade leads to a 10 dB OSNR degradation after 32 cascaded ROADMs and should be considered as a limitation factor to the number of ROADMs that a signal can cross in an optical network.

ACKNOWLEDGEMENTS

This work was supported by Fundação para a Ciência e Tecnologia (FCT) of Portugal within the project UID/EEA/50008/2013.

REFERENCES

Cancela, L., et al. (2016). Analytical tools for evaluating the impact of in-band crosstalk in DP-QPSK signals. *NOC,* 6-11.

Colbourne, P. and Collings, B. (2011), ROADM Switching Technologies. *OFC*, pp. OTuD1.

Essiambre, R., (2010). Capacity limits of optical fiber networks. *J. Lightw. Technol.*, *28*(4), 662-701.

Feuer, M., et al. (2011). Intra-node contention in dynamic photonic networks. *J. Lightw. Technol.*, *29*(4), 529-535.

Filer, M. and Tibuleac, S. (2012). Generalized weighted crosstalk for DWDM systems with cascaded wavelength-selective switches. *Opt. Exp.*, *20*(16), 17620-17631.

Filer, M. and Tibuleac, S. (2014). N-degree ROADM architecture comparison: Broadcast-and-select versus route-and-select in 120 Gb/s DP-QPSK transmission systems. *OFC,* pp. Th1I-2.

Gringeri, S., et al. (2010). Flexible architectures for optical transport nodes and networks. *IEEE Commun. Mag.*, *48*(7), 40-50.

Hsueh, Y., et al. (2012). Passband narrowing and crosstalk impairments in ROADM-enabled 100G DWDM networks. *J. Lightw. Technol.*, *30*(24), 3980-3986.

Jinno, M. (2017). Elastic optical networking: Roles and benefits in beyond 100-Gb/s era. *J. Lightw. Technol., 35*(5), 1116-1124.

Morea, A., et al. (2015). Throughput comparison between 50-GHz and 37.5-GHz grid transparent networks. *J. Opt. Commun. Netw., 7*(2), A293-A300.

Pan, J. and Tibuleac, S. (2016). Filtering and crosstalk penalties for PDM-8QAM/16QAM super-channels in DWDM networks using broadcast-and-select and route-and-select ROADMs. *OFC*, pp. W2A-49.

Pulikkaseril, C. (2011). Spectral modeling of channel band shapes in wavelength selective switches. *Opt. Exp.*, *19*(9), 8458-8470.

Roberts, K., et al. (2017). Beyond 100 Gb/s: capacity, flexibility, and network optimization. *J. Opt. Commun. Netw., 9*(4), C12-C24.

Seimetz, M. and Weinert, C. (2006). Options, feasibility, and availability of 2×4 90º hybrids for coherent optical systems. *J. Lightw. Technol.*, *24*(3), 1317-1322.

Simmons, J. (2014). *Optical network design and planning*. Springer, 2nd edition.

Tibuleac, S. and Filer, M. (2010). Transmission impairments in DWDM networks with reconfigurable optical add-drop multiplexers. *J. Lightw. Technol.*, *28*(4), 557-598.

Way, W. (2012). Optimum architecture for M×N multicast switch-based colorless, directionless, contentionless, and flexible-grid ROADM. *OFC*, pp. NW3F-5.

Woodward, S., et al., (2010). Intra-node contention in a dynamic, colorless, non-directional ROADM. *OFC*.

Yang, H., et al. (2017). Low-cost CDC ROADM architecture based on stacked wavelength selective switches. *J. Opt. Commun. Netw.*, *9*(5), 375-384.

Zami, T. (2013). Current and Future Flexible Wavelength Routing Cross-Connects. *Bell Labs Technical Journal*, *18*(3), 23-38.